Journal of Food and Drug Analysis

Volume 33 | Issue 3 Article 9

Anti-neuroinflammatorypolyketides from the medicinal herb-derived fungal strain Didymocyrtis brachylaenae Km1530

Recommended Citation
Chang, Chia-Hao; Zhang, Yun-Rong; Huang, Shu-Jung; Hsiao, George; Chi, Wei-Chiung; Gu, Andrea; Lai, Yu-Wei; and Lee, Tzong-Huei (2025) "Anti-neuroinflammatorypolyketides from the medicinal herb-derived fungal strain Didymocyrtis brachylaenae Km1530," *Journal of Food and Drug Analysis*: Vol. 33 : Iss. 3 , Article 9.
Available at: https://doi.org/10.38212/2224-6614.3560

ORIGINAL ARTICLE

Anti-neuroinflammatory polyketides from the medicinal herb-derived fungal strain *Didymocyrtis brachylaenae* Km1530

Chia-Hao Chang [a], Yun-Rong Zhang [a], Shu-Jung Huang [a], George Hsiao [b,c], Wei-Chiung Chi [d], Andrea Gu [a], Yu-Wei Lai [e], Tzong-Huei Lee [a,f,*]

[a] Institute of Fisheries Science, College of Life Science, National Taiwan University, Taipei 106319, Taiwan
[b] Department of Pharmacology, School of Medicine, Taipei Medical University, Taipei 110301, Taiwan
[c] Graduate Institute of Medical Sciences, College of Medicine, Taipei Medical University, Taipei 110301, Taiwan
[d] Department of Food Science, National Quemoy University, Kinmen 892009, Taiwan
[e] Center of General Education, National Taipei University, New Taipei 273303, Taiwan
[f] Department of Life Science, College of Life Science, National Taiwan University, Taipei 106319, Taiwan

Abstract

A series of chromatographic separation on the liquid-state fermented products of *Didymocyrtis brachylaenae* Km1530 derived from the littoral medicinal herb *Atriplex maximowicziana* Makino, resulted in the isolation of compounds 1−13. Their structures were determined by spectroscopic analysis as five previously unreported C_{13} polyketides, namely brachylactones A−D (1−4) and brachic acid (5), along with eight known compounds 6−13. Among these, brachylactones A (1) and B (2) exhibited nitric oxide production inhibitory activity in lipopolysaccharide-induced murine BV-2 microglial cells at a concentration of 20 μM without any cytotoxicity.

Keywords: Anti-neuroinflammation, Brachylactone, *Didymocyrtis brachylaenae*, Nitric oxide, Polyketide

1. Introduction

Since endophytes were first described in 1809 by the German plant scientist Heinrich Friedrich Link, their definition has undergone numerous revisions. They are widely recognized as microorganisms that spend part or all of their life cycles within the healthy tissues of host plants, without causing any apparent symptoms of disease. [1−5]. Endophytic fungi are supported and protected by the host plants under the symbiotic relationship, and in return, the microorganisms produce bioactive specialized metabolites to defend the plants from pathogens and herbivores or accelerating the growth of the host plants [6,7]. Especially, the host plants living in extreme environments might prompt the endophytic fungi to activate silent genes and induce unique biosynthetic gene expression for producing distinctive natural products with novel structures and particular mechanisms to survive under stress conditions [8,9]. Therefore, the attention of natural product researchers has been increasingly attracted to endophytic fungi from special environments for the sources of leading drug candidates [10,11]. According to the statistical results of the literature, the number of new compounds produced by marine fungi has gradually increased from 2016 to 2019, especially accounted for 50% of the total in 2019 [12].

The littoral plant *Atriplex maximowicziana* Makino (Chenopodiaceae) is distributed widely at sandy soils and coral-rocky seashores of Southeast China, Southern Japan, and Southwest Taiwan [13]. It has long been used as folk medicines for treating rheumatoid arthritis [13,14]. Given that it thrives in a challenging environment characterized by intense sunlight, strong tides, drastic salinity fluctuations,

Received 14 October 2024; accepted 4 August 2025.
Available online 18 September 2025

* Corresponding author at: Institute of Fisheries Science, National Taiwan University, No.1, Sec. 4, Roosevelt Rd., Da'an Dist., Taipei 106319, Taiwan.
E-mail address: thlee1@ntu.edu.tw (T.-H. Lee).

https://doi.org/10.38212/2224-6614.3560

and microbial infections, it is speculated that the presence of highly diverse endophytic fungi may serve as a crucial strategy, producing bioactive compounds to help the host withstand these harsh conditions [15,16].

In this study, the fungal strain *Didymocyrtis brachylaenae* Km1530 (Phaeosphaeriaceae) was isolated from the leaves of *A. maximowicziana* Makino. The fungal strain was cultured in PDY media and then furnished the crude extracts that exhibited significant anti-inflammatory activity at a concentration of 100 μg/mL in a preliminary biological evaluation. In literatures, the one strain many compounds (OSMAC) strategy has been proven to be a pleiotropic method for affecting the expression of multiple genes simultaneously at different levels, which can be employed physically or chemically to activate the silent or cryptic gene clusters for enhancing chemodiversity of secondary metabolites with both medical and biotechnological interests [17–19]. To date, the OSMAC has been recognized as a highly effective and widely adopted method in fungal natural product research, enabling natural product chemists to explore metabolic diversity without the need for genetic manipulation [20]. Thus, the chemical constituents of *D. brachylaenae* Km1530 was investigated intensively by applying OSMAC strategy. Consequently, five previously undescribed C_{13}-polyketides, brachylactones A–D (**1**–**4**) and brachic acid (**5**) (Fig. 1), together with eight known compounds have been isolated and identified. Herein, the isolation and structural characterization of previously unreported compounds was discussed along with their nitric oxide (NO) production inhibitory activity in lipopolysaccharide-induced murine microglial BV-2 cells.

2. Materials and methods

2.1. General experimental procedures

HRESIMS were measured on a Q Extractive Plus Hybrid Quadrupole-Orbitrap Mass Spectrometer (Thermo Fisher Scientific, Bremen, Germany). Optical rotations were recorded on a JASCO P-2000 digital polarimeter (JASCO, Tokyo, Japan). UV spectra were obtained on a Thermo UV–visible Heλios α spectrophotometer (Bellefonte, CA, USA). IR spectra were received on a JASCO FT/IR 4100 spectrometer (Tokyo, Japan). NMR spectra were measured on a Bruker AVIII 500 MHz FT-NMR spectrometer (Bruker BioSpin GmbH, Ettlingen, Germany). HPLC purification was performed on a Hitachi D-2000 system (Hitachi, Tokyo, Japan) coupled with an L-7100 pump (Hitachi, Tokyo, Japan), and Bischoff RI-8120 detector (Bischoff, Leonberg, Germany), and equipped with a Phenomenex Luna column (PFP, 5 μ, 10 i.d. × 250 mm) (Phenomenex, Torrance, CA, USA), and a Kinetex column (XB-C18, 5 μ, 4.6 i.d. × 250 mm) (Phenomenex, Torrance, CA, USA). MPLC was performed on a SepaBean machine U200 (SepaBean®, Changzhou, China) coupled with a Sepaflash™ Ruby column (Spherical Silica, 15 μ, 50 Å, 25 g) (SepaBean®, Changzhou, China). Open column chromatography

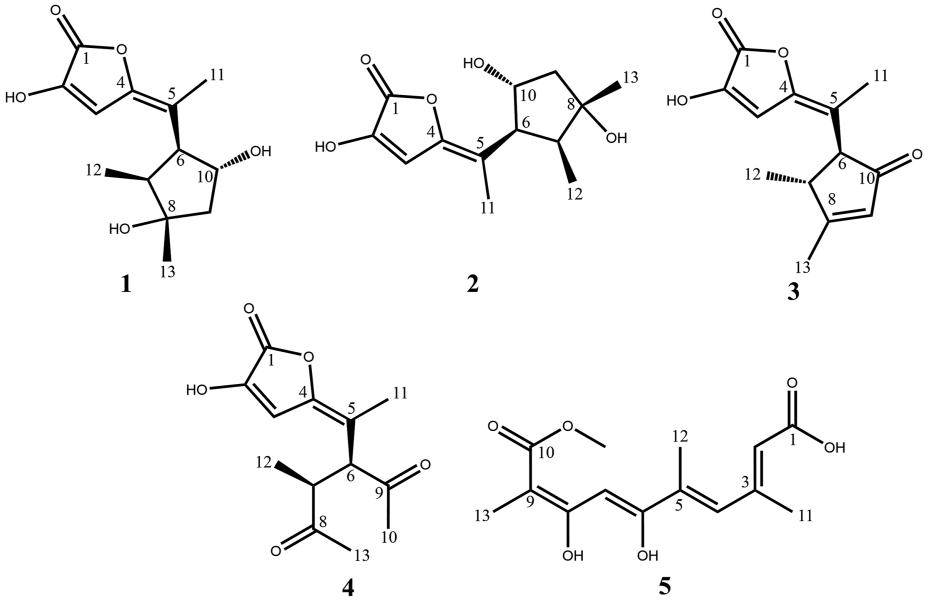

*Fig. 1. Chemical structures of compounds **1**–**5** isolated in this study.*

was performed using Sephadex LH-20 (2.5 i. d. × 67.0 cm) (Sigma-Aldrich, St. Louis, MO, USA). TLC was carried out with precoated silica gel 60 F_{254} (Merck, Darmstadt, Germany). Compounds were detected by UV 254 nm irradiation and 10% aqueous H_2SO_4 spraying reagent followed by heating at 105 °C for 30 s. The solvents were LC grade methanol (Merck, Darmstadt, Germany) for HPLC purification, AR grade *n*-hexane, acetone, methanol (Merck, Darmstadt, Germany), and ethyl acetate (Duksan, Ansan, Korea) for extraction and MPLC and open column elution, and methanol-d_4 (Sigma-Aldrich, St. Louis, MO, USA) and pyridine-d_5 (Sigma-Aldrich, St. Louis, MO, USA) for NMR acquisition.

2.2. Fungal strain and culture

The fungal strain *Didymocyrtis brachylaenae* Km1530 was isolated from a fresh leaf of *Atriplex maximowicziana* Makino that was collected from Kinmen County (24°27′04.0″N118°15′06.5″E), Taiwan, in November 2017. The fungal strain was identified according to morphological characteristics and the molecular biology method using the 28S rRNA gene sequence. The sequence data for this strain have been deposited in GenBank with the accession number PP388219. The purified strain was initially cultivated on PDA medium (Becton, Dickinson and Company, Sparks, MD, USA) at 26 °C for 7 days. The resulting agar culture was cut into small cubes (approximately 1 × 1 × 1 cm^3) and transferred into 250 mL flasks containing 100 mL of different seed media (ME, PDY, and PDB), each sterilized at 121 °C for 20 min and incubated at 26 °C with shaking at 180 rpm for 7 days.

For the ME group, the medium consisted of 20 g of malt extract (Becton, Dickinson and Company, Sparks, MD, USA) per liter of seawater. After initial cultivation, the seed broth was transferred into 10 × 5 L bottles, each containing 3.5 L of the same malt extract medium, and incubated at 26 °C under aeration for 20 days. The seawater used was collected from the northeastern coast of Taiwan, filtered prior to use, and had a salinity of 35‰, measured using a salinometer; for the PDY group, the medium consisted of 10 g dextrose (Sigma-Aldrich, St. Louis, MO, USA), 2 g peptone (Becton, Dickinson and Company, Sparks, MD, USA), and 1 g yeast extract (Becton, Dickinson and Company, Sparks, MD, USA) per liter of seawater. The resulting seed culture was inoculated into 72 × 250 mL flasks, each containing 100 mL of the same PDY medium, and cultured at 26 °C with shaking at 180 rpm for 20 days; for the PDB group, the medium was prepared using 24 g of PDB powder (Becton, Dickinson and Company, Sparks, MD, USA) per liter of distilled water. Following the initial cultivation, the seed broth was transferred into 10 × 5 L bottles, each containing 3.5 L of the same PDB medium, and cultured at 26 °C under aeration for 20 days.

2.3. Extraction and isolation of secondary metabolites

The fermented ME broth (35.0 L) was filtered, the filtrate was extracted with EtOAc (2 × 35.0 L), and the resulting extract was evaporated under reduced pressure to afford a viscous solid (1.9 g), which was absorbed by spherical silica gel (25 μm, 50 Å, 12 g) and applied to MPLC eluted with *n*-hexane : acetone in the ratio of 4:1 (v : v) for 5 min, *n*-hexane : acetone in the ratio of 3:1 (v : v) for 7.5 min, *n*-hexane : acetone in the ratio of 2:1 (v : v) for 7.5 min, *n*-hexane : acetone in the ratio of 1:1 (v : v) for 7.5 min, 100% acetone for 5 min, and 100% methanol for 10 min to afford 20 fractions (MI–MXX) based on TLC analyses. Fraction MVII was further purified by semipreparative HPLC using a Phenomenex Luna PFP column (5 μm, 100 Å, 250 × 10 mm) with 35% MeOH/H_2O containing 0.1% formic acid (2.0 mL/min) as eluent to obtain **8** (6.7 mg, t_R = 29.3 min). Fraction MIX was further purified by semipreparative HPLC using a Phenomenex Luna PFP column (5 μm, 100 Å, 250 × 10 mm) with 60% MeOH/H_2O containing 0.1% formic acid (2.0 mL/min) as mobile phase to give **7** (10.1 mg, t_R = 8.5 min). Fraction MXII was further purified by semipreparative HPLC using a Phenomenex Luna PFP column (5 μm, 100 Å, 250 × 10 mm) with 45% MeOH/H_2O containing 0.1% formic acid (2.0 mL/min) as eluent to yield **3** (8.4 mg, t_R = 25.7 min) and mixture (t_R = 20.8 min), and then was further clarified by analytical HPLC using a Kinetex XB-C18 (5 μm, 250 × 4.6 mm) with 40% MeOH/H_2O containing 0.1% formic acid (1.0 mL/min) as mobile phase to yield **4** (4.9 mg, t_R = 8.4 min). Fraction MXIV was further purified by semipreparative HPLC using a Phenomenex Luna PFP column (5 μm, 100 Å, 250 × 10 mm) with 50% MeOH/H_2O containing 0.1% formic acid (2.0 mL/min) as eluent to afford **1** (63.9 mg, t_R = 12.6 min), **2** (36.8 mg, t_R = 13.9 min), and **6** (6.0 mg, t_R = 41.8 min). The fermented PDY broth (7.2 L) was filtered, the filtrate was extracted with EtOAc (2 × 7.2 L), and the resulting extract was evaporated under reduced pressure to afford a viscous solid (0.3 g). The crude extract was initially purified by semipreparative HPLC using a Phenomenex Luna PFP column (5 μm, 100 Å, 250 × 10 mm) with 30%

MeOH/H_2O containing 0.1% formic acid (2.0 mL/min) as eluent to obtain mixture (t_R = 31.7 min), and then was further clarified by analytical HPLC using a Kinetex XB-C18 (5 μm, 250 × 4.6 mm) with 20% MeOH/H_2O containing 0.1% formic acid (1.0 mL/min) as mobile phase to yield **9** (5.2 mg, t_R = 12.1 min). The fermented PDB broth (35.0 L) was filtered, the filtrate was extracted with EtOAc (2 × 35.0 L), and the resulting extract was evaporated under reduced pressure to afford a viscous solid (1.8 g), which was applied to a Sephadex LH-20 column (2.5 i.d. × 67.0 cm) eluted with MeOH, to afford 11 fractions (PI–PXI) based on TLC analyses. Fraction PV was further purified by semi-preparative HPLC using a Phenomenex Luna PFP column (5 μm, 100 Å, 250 × 10 mm) with 60% MeOH/H_2O containing 0.1% formic acid (2.0 mL/min) as eluent to obtain **5** (6.7 mg, t_R = 31.7 min) and a mixture (t_R = 9.3 min), which was further purified by the same column with 40% MeOH/H_2O containing 0.1% formic acid (2.0 mL/min) to furnish **11** (9.9 mg, t_R = 16.6 min). Fraction PVI was further purified by semipreparative HPLC using a Phenomenex Luna PFP column (5 μm, 100 Å, 250 × 10 mm) with 40% MeOH/H_2O containing 0.1% formic acid (2.0 mL/min) as eluent to obtain **10** (9.5 mg, t_R = 33.8 min) and a mixture (t_R = 16.5 min), which was further purified by the same column with 25% MeOH/H_2O containing 0.1% formic acid (2.0 mL/min) to give **12** (17.7 mg, t_R = 12.7 min). Fraction PVII was further purified by semi-preparative HPLC using a Phenomenex Luna PFP column (5 μm, 100 Å, 250 × 10 mm) with 45% MeOH/H_2O containing 0.1% formic acid (2.0 mL/min) as eluent to obtain **13** (14.9 mg, t_R = 24.1 min).

*Table 1. ^{13}C NMR spectroscopic data for compounds **1**–**5** (δ in ppm).*

No.	1 [a]	2 [a]	3 [a]	4 [a]	5 [b]
1	168.2	168.2	167.7	167.3	169.3
2	145.6	145.7	146.7	147.6	123.2
3	110.5	110.3	109.6	109.4	151.4
4	146.6	145.9	147.1	147.9	134.8
5	122.7	122.0	116.7	114.5	129.9
6	50.7	49.4	58.8	57.9	159.6
7	48.2	48.2	46.0	47.1	95.4
8	79.2	79.3	186.0	213.2	166.3
9	50.8	51.0	130.8	207.2	103.4
10	75.6	75.4	209.8	29.9	164.6
11	16.9	17.2	12.3	12.4	19.5
12	10.8	11.0	17.4	16.1	14.4
13	29.6	29.8	17.5	29.2	9.7
10-OCH_3					56.9

[a] Measured in methanol-d_4 (125 MHz).
[b] Measured in pyridine-d_5 (125 MHz).

2.3.1. Brachylactones A (1)

Yellowish powder; $[\alpha]_D^{25}$ +182.4 (*c* 0.5, MeOH); UV (MeOH) λ_{max} (log ε) 297 (4.17) nm; IR (ATR) ν_{max} 3402, 2962, 1743, 1616, 1246, 1103, 930, 833 cm^{-1}; ^1H NMR data (methanol-d_4, 500 MHz) see Table 2; ^{13}C NMR data (methanol-d_4, 125 MHz) see Table 1; HRESIMS *m/z* 237.1122 $[M - H_2O + H]^+$ (calcd. 237.1127 for $C_{13}H_{17}O_4$) and 253.1069 $[M - H]^-$ (calcd. 253.1076 for $C_{13}H_{17}O_5$).

2.3.2. Brachylactones B (2)

Yellowish powder; $[\alpha]_D^{25}$ +183.8 (*c* 0.5, MeOH); UV (MeOH) λ_{max} (log ε) 301 (4.23) nm; IR (ATR) ν_{max} 3390, 2958, 2681, 1739, 1616, 1442, 1389, 1261, 1091, 833 cm^{-1}; ^1H NMR data (methanol-d_4, 500 MHz) see Table 2; ^{13}C NMR data (methanol-d_4, 125 MHz) see Table 1; HRESIMS *m/z* 237.1123 $[M - H_2O + H]^+$ (calcd. 237.1127 for $C_{13}H_{17}O_4$) and 253.1070 $[M - H]^-$ (calcd. 253.1076 for $C_{13}H_{17}O_5$).

*Table 2. ^1H NMR spectroscopic data for compounds **1**–**5** [δ (in ppm) mult. (J in Hz)].*

No.	1 [a]	2 [a]	3 [a]	4 [a]	5 [b]
1					
2					6.21 q (2.3)
3	6.70 s	6.71 s	6.69 s	6.87 s	
4					7.11 brs
5					
6	3.21 dd (6.5, 9.5)	3.71 dd (6.5, 9.5)	3.08 d (3.5)	3.86 d (11.0)	
7	2.10 qd (7.5, 9.5)	2.16 qd (7.5, 9.5)	2.85 dq (3.5, 7.0)	3.31 qd (7.0, 11.0)	6.42 s
8					
9	2.04 dd (6.5, 13.5)	2.03 dd (6.5, 13.5)	6.00 s		
	2.10 dd (6.5, 13.5)	2.09 dd (6.5, 13.5)			
10	4.32 q (6.5)	4.34 q (6.5)		2.13 s	
11	2.14 s	2.08 s	1.70 s	1.73 s	2.46 dd (0.9, 2.3)
12	0.90 d (7.5)	0.89 d (7.5)	1.26 d (7.0)	1.11 d (7.0)	2.01 d (2.0)
13	1.30 s	1.30 s	2.19 s	2.10 s	2.13 s
10-OCH_3					3.83 s

[a] Measured in methanol-d_4 (500 MHz).
[b] Measured in pyridine-d_5 (500 MHz).

2.3.3. Brachylactones C (3)

Yellowish powder; $[\alpha]_D^{25}$ −12.6 (*c* 0.1, MeOH); UV (MeOH) λ_{max} (log ε) 228 (3.84), 294 (3.81) nm; IR (ATR) ν_{max} 3113, 2966, 1755, 1685, 1612, 1439, 1381, 1257, 1180, 1089 cm^{-1}; ^1H NMR data (methanol-d_4, 500 MHz) see Table 2; ^{13}C NMR data (methanol-d_4, 125 MHz) see Table 1; HRESIMS *m/z* 235.0966 $[M + H]^+$ (calcd. 235.0970 for $C_{13}H_{15}O_4$) and 233.0813 $[M - H]^-$ (calcd. 233.0814 for $C_{13}H_{13}O_4$).

2.3.4. Brachylactones D (4)

Yellowish powder; $[\alpha]_D^{25}$ −160.8 (*c* 0.1, MeOH); UV (MeOH) λ_{max} (log ε) 288 (3.99), 310 (3.94) nm; IR (ATR) ν_{max} 3116, 2935, 1759, 1709, 1624, 1373, 1238, 1165, 1092, 957, 833 cm^{-1}; ^1H NMR data (methanol-d_4, 500 MHz) see Table 2; ^{13}C NMR data (methanol-d_4, 125 MHz) see Table 1; HRESIMS *m/z* 253.1071 $[M + H]^+$ (calcd. 253.1076 for $C_{13}H_{17}O_5$) and 251.0918 $[M - H]^-$ (calcd. 251.0919 for $C_{13}H_{15}O_5$).

2.3.5. Brachic acid (5)

Yellowish powder; UV (MeOH) λ_{max} (log ε) 218 (4.35), 263 (4.16), 343 (4.17) nm; IR (ATR) ν_{max} 3336, 2939, 2835, 1658, 1412, 1111, 1018 cm^{-1}; ^1H NMR data (pyridine-d_5, 500 MHz) see Table 2; ^{13}C NMR data (pyridine-d_5, 125 MHz) see Table 1; HRESIMS *m/z* 265.1065 $[M - H_2O + H]^+$ (calcd. 265.1076 for $C_{14}H_{17}O_5$) and 263.0927 $[M - H_2O - H]^-$ (calcd. 263.0919 for $C_{14}H_{15}O_5$).

2.4. Cell culture

The murine microglial cell line BV-2 was cultured as described previously [21]. Before experiments, a confluence of 85% of cells were changed to 0.5% FBS media. Thereafter, cells were treated with vehicle or the indicated concentration of compounds **1**–**13** for 15 min and then stimulated with LPS (150 ng/mL) for 24 h. The conditioned medium was freshly collected and frozen at −80 °C.

2.4.1. Cell viability

The viability of the BV-2 cells was determined by the MTT method. Approximately 1×10^5 cells were seeded in 24-well plates per well and grown for 24 h before use. Then, the cells were pretreated with test compounds at 20 μM for 24 h [22]. The final concentration of DMSO in the culture medium of the treated cells was adjusted to less than 0.5% (v/v) to prevent a solvent effect. DMSO was also treated as a vehicle control. The absorbance was checked at 550 nm was obtained by a microplate reader (MRX). All of the experiments were performed in triplicate.

2.4.2. Assay for nitric oxide (NO) inhibitory activity

NO inhibitory activity of selected compounds was evaluated by using an LPS-induced cell model. Production of NO was evaluated by measuring the levels of nitrite in a conditioned medium as previously described with some modification. The treated concentrations of test compounds, cell culture plates, and positive control (curcumin) were modified in this study [23]. The culture supernatants were allowed to react with reconstituted cofactor solution and reconstituted nitrate reductase solution for 10 min at room temperature in the dark according to the manufacturer's instructions of the nitrate/nitrite colorimetric assay kit (Cayman). Absorptions were measured at 550 nm using a microplate reader (MRX). Nitrite concentrations were calculated from the standard solutions of sodium nitrite.

*2.5. Preparation of (S)- and (R)-MTPA esters of **1** and **2***

Compounds **1** and **2** (each 0.5 mg) were dissolved in 500 μL of pyridine-d_5. Then, 5 μL of (*S*)- or (*R*)-α-methoxy-α-trifluoromethylphenylacetyl chloride (MTPA-Cl) was added to the above solutions, which were allowed to react at room temperature for 4 h. The mixtures were subjected to measurement of a 500 MHz NMR spectrometer [24–26].

3. Results and discussion

The EtOAc extracts of fermented broths of *D. brachylaenae* Km1530 were fractionated and purified sequentially by column chromatography on Sephadex LH-20 or MPLC and followed by semi-preparative HPLC to yield undescribed compounds **1**–**5** as well as eight known compounds **6**–**13**.

Compound **1** was obtained as yellowish powder, and was determined to have the molecular formula $C_{13}H_{18}O_5$ as deduced from a dehydrated pseudo-molecular ion $[M - H_2O + H]^+$ at *m/z* 237.1122 (calcd. 237.1127 for $C_{13}H_{17}O_4$) and a deprotonated molecular ion $[M - H]^-$ at *m/z* 253.1069 (calcd. 253.1076 for $C_{13}H_{17}O_5$) in the HRESIMS, as supported by analysis of ^{13}C NMR data of **1** (Table 1), indicating five degrees of unsaturation. Its IR spectrum displayed absorption bands at 3402 and 1743 cm^{-1}, revealing the presence a hydroxy and a conjugated γ-lactone moiety, respectively. The ^1H NMR spectrum of **1** showed signals for three methyls at δ_H 0.90 (3H, d, J = 7.5 Hz, H_3-12), 1.30 (3H, s, H_3-13), and 2.14 (3H, s, H_3-11), one methylene at δ_H 2.04 (1H, dd, J = 6.5, 13.5 Hz, H_a-9) and 2.10 (1H, dd, J = 6.5, 13.5 Hz, H_b-9), two aliphatic methines at δ_H 2.10 (1H, qd,

J = 7.5, 9.5 Hz, H-7) and 3.21 (1H, dd, J = 6.5, 9.5 Hz, H-6), one olefinic protons at δ_H 6.70 (1H, s, H-3), and one carbinoyl methine at δ_H 4.32 (H, q, J = 6.5 Hz, H-10) (Table 2). Interpretation of the ^{13}C NMR accompanied by phase-sensitive HSQC spectra revealed 13 carbon signals attributable to three methyls at δ_C 10.8 (C-12), 16.9 (C-11), and 29.6 (C-13), one methylene at δ_C 50.8 (C-9), three aliphatic methines at δ_C 48.2 (C-7), 50.7 (C-6), and 75.6 (C-10), one olefinic methine at δ_C 110.5 (C-3), and five nonprotonated carbons at δ_C 79.2 (C-8), 122.7 (C-5), 145.6 (C-2), 146.6 (C-4), and 168.2 (C-1) (Table 1). Among, these, two distinctive signals at δ_C 75.6 (C-10) and 168.2 (C-1) were assigned to be carbinoyl carbon and lactone carbonyl carbon, respectively. Cross-peaks of H-6/H-7; H-6/H-10; H-7/H_3-12; and H_2-9/H-10 in the COSY spectrum together with key cross-peaks of H-3/C-1, -2, and -4; H-6/C-4 and -5; H_2-9/C-6, -8, and -10; H_3-11/C-4, -5, and -6; H_3-12/C-6, -7, and -8; and H_3-13/C-7, -8, and -9 in the HMBC spectrum (Fig. 2) confirmed the planar structure of **1** as shown. Based on the key cross-peaks of H-3/H-6; H-10/H_3-11 and -13; and H_3-11/H_3-12 and -13 in the NOESY spectrum (Fig. 2), the configuration of $\Delta^{4(5)}$ was deduced to be *E* form, and the relative stereochemistry of H-6, H-10, H_3-12, and H_3-13 were determined to be α-, β-, β-, and β-oriented, respectively. In order to establish the absolute configuration of **1**, the modified Mosher's method was applied to observe the differences in chemical shifts ($\Delta\delta = \delta_S - \delta_R$) of *S*/*R*-MTPA-derivatives (Fig. 3), indicating the absolute configuration of C-6, -7, -8, and -10 in **1** is *S*, *S*, *S*, and *R*, respectively.

The HRESIMS of compound **2** showed a dehydrated pseudo-molecular ion peak at *m/z* 237.1123 $[M - H_2O + H]^+$ (calcd. 237.1127 for $C_{13}H_{17}O_4$) and a deprotonated molecular ion at *m/z* 253.1070 $[M - H]^-$ (calcd. 253.1076 for $C_{13}H_{17}O_5$). When comparing the ^1H and ^{13}C NMR data of **2** with those of pestalotiolactone B [27], they were almost consistent except that δ_C 48.9 (C-6) in pestalotiolactone B shifted apparently to δ_C 49.4 in compound **2** (Table S1 https://doi.org/10.38212/2224-6614.3560), suggesting **2** was a stereoisomer of pestalotiolactone B. Key cross-peaks of H-3/H_3-11; H_3-11/H-10, H_3-12, and -13; and H_3-12/H_3-13 in the NOESY spectrum of **2** (Fig. 2) established the relative configuration of **2** as shown. The absolute configurations of **2** were assigned as 6*S*, 7*S*, 8*S*, and 10*R* based on the chemical shift differences of *S*/*R*-MTPA-esters of **2** (Fig. 3).

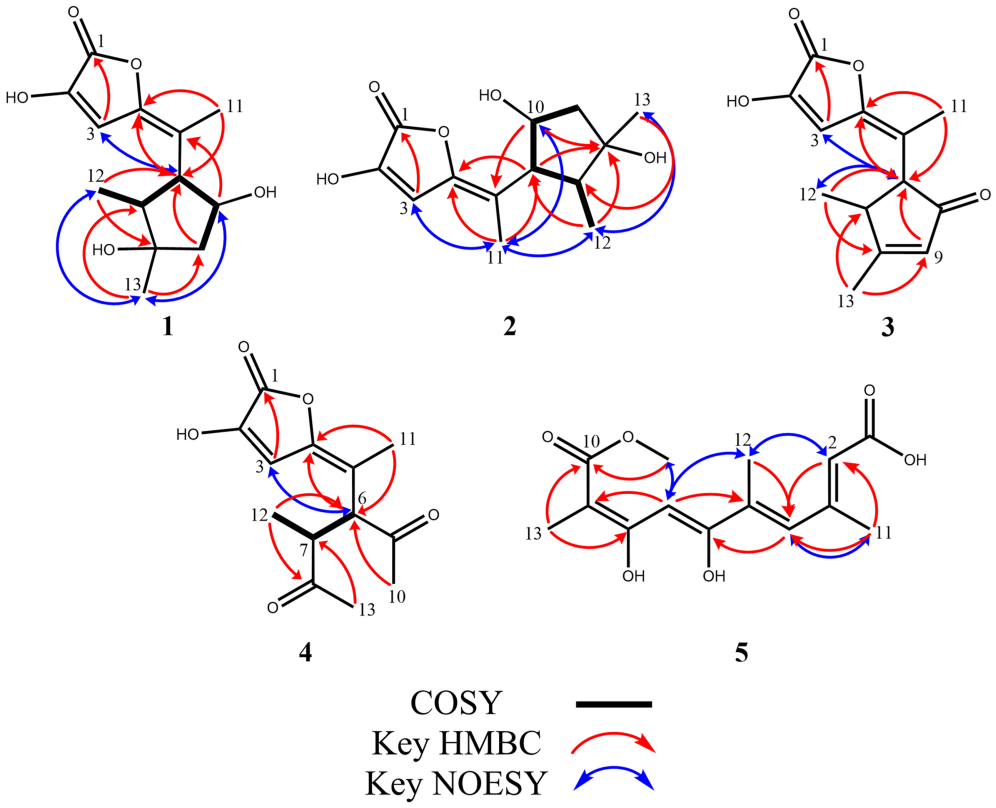

*Fig. 2. COSY, key HMBC, and NOESY correlations of compounds **1**–**5**.*

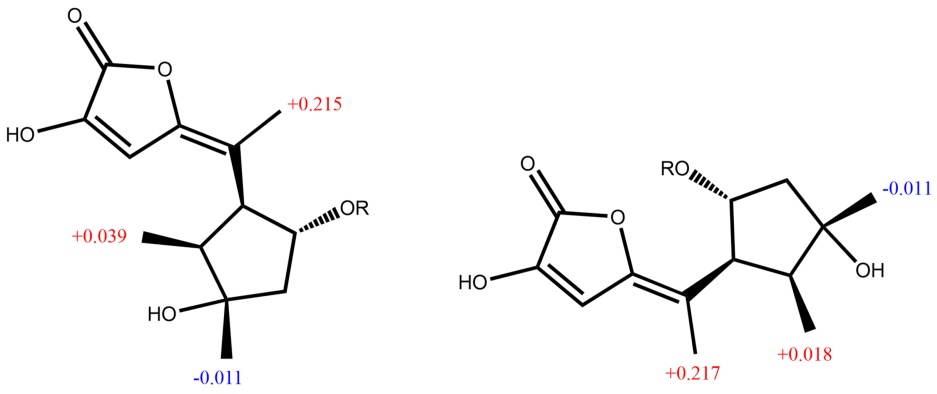

1a: R = (*S*)-MTPA
1b: R = (*R*)-MTPA

2a: R = (*S*)-MTPA
2b: R = (*R*)-MTPA

*Fig. 3. $\Delta\delta_{S\text{-}R}$ values (in ppm) of ^{1}H NMR obtained from (S)- and (R)-MTPA esters of compounds **1** and **2** in pyridine-d_5 (500 MHz).*

Compound **3** was deduced to have a chemical formula of $C_{13}H_{14}O_4$ by HRESIMS of a protonated ion peak at *m/z* 235.0966 $[M + H]^+$ (calcd. 235.0970 for $C_{13}H_{15}O_4$) as well as a deprotonated molecular ion at *m/z* 233.0813 $[M - H]^-$ (calcd. 233.0814 for $C_{13}H_{13}O_4$). The IR spectrum displayed absorptions at 3113, 1755, and 1685 cm^{-1}, indicating the presence of a hydroxy group, a conjugated γ-lactone, and a conjugated ketone group. The ^{1}H NMR spectrum of **3** showed signals for three methyls at δ_H 1.26 (3H, d, J = 7.0 Hz, H_3-12), 1.70 (3H, s, H_3-11), and 2.19 (3H, s, H_3-13), two aliphatic methines at δ_H 2.85 (1H, dq, J = 3.5, 7.0 Hz, H-7) and 3.08 (1H, d, J = 3.5 Hz, H-6), and two olefinic methines at δ_H 6.00 (1H, s, H-9) and 6.69 (1H, s, H-3) (Table 2). Interpretation of the ^{13}C NMR supported by HSQC spectrum revealed 13 carbon signals including three methyls at δ_C 12.3 (C-11), 17.4 (C-12), and 17.5 (C-13), two aliphatic methines at δ_C 46.0 (C-7) and 58.8 (C-6), two olefinic methines at δ_C 109.6 (C-3) and 130.8 (C-9), and six nonprotonated carbons at δ_C 116.7 (C-5), 146.7 (C-2), 147.1 (C-4), 167.7 (C-1), 186.0 (C-8), and 209.8 (C-10) (Table 1). Of these assignments, the conspicuous signals at δ_C 167.7 (C-1) and 209.8 (C-10) were assigned to be a lactone carbonyl group and a ketone carbonyl functionality, respectively. Cross-peaks of H-6/H-7 and H-7/H_3-12 in the COSY spectrum and key correlations of H-3/C-1 and -4; H-6/C-4 and -12; H-7/C-8; H-9/C-6 and -8; H_3-11/C-4, -5, and -6; H_3-12/C-6, -7, and -8; and H_3-13/C-7, -8, and -9 in the HMBC spectrum (Fig. 2) confirmed the plain structure of compound **3**. On the basis of key cross-peaks of H-3/H-6 and H-6/H_3-12 in the NOESY spectrum of **3** (Fig. 2), the configuration of $\Delta^{4(5)}$ was deduced to be *E* form and the relative configurations of C-6 and C-7 in **3** were concluded to be *S** and *R**, respectively.

The HRESIMS of compound **4** revealing a protonated molecular ion peak at *m/z* 253.1071 $[M + H]^+$ (calcd. 253.1076 for $C_{13}H_{17}O_5$) and a deprotonated molecular ion at *m/z* 251.0918 $[M - H]^-$ (calcd. 251.0919 for $C_{13}H_{15}O_5$) allowed the assignment of its molecular formula to be $C_{12}H_{16}O_5$. The IR spectrum showed absorptions at 3116, 1759, and 1708 cm^{-1}, indicating the presence of a hydroxy group, a conjugated γ-lactone, and a ketone group. The ^{1}H NMR spectrum displayed signals for four methyls at δ_H 1.11 (3H, d, J = 7.0 Hz, H_3-12), 1.73 (3H, s, H_3-11), 2.10 (3H, s, H_3-13), and 2.13 (3H, s, H_3-10), two aliphatic methines at δ_H 3.31 (1H, qd, J = 7.0, 11.0 Hz, H-7) and 3.86 (1H, d, J = 11.0 Hz, H-6), and one olefinic proton at δ_H 6.87 (1H, s, H-3) (Table 2). The ^{13}C NMR accompanied with HSQC spectra of **4** showed 13 resonances, which were ascribed to four methyls at δ_C 12.4 (C-11), 16.1 (C-12), 29.2 (C-13), and 29.9 (C-10), two aliphatic methines at δ_C 47.1 (C-7) and 57.9 (C-6), one olefinic methine at δ_C 109.4 (C-3), and six nonprotonated carbons at δ_C 114.5 (C-5), 147.6 (C-2), 147.9 (C-4), 167.3 (C-1), 207.2 (C-9), and 213.2 (C-8). Among these, the signals at δ_C 167.3 (C-1) was assigned to γ-lactone carbonyl group, and both the signals at δ_C 207.2 (C-9) and 213.2 (C-8) were deduced as ketone carbonyl functionalities. Correlations of H-6/H-7 and H-7/H_3-12 in the COSY spectrum and key correlations of H-3/C-1 and -4; H-6/C-4 and -5; H-7/C-8; H_3-10/C-6 and -9; H_3-11/C-4, -5, and -6; H_3-12/C-6, -7, and -8; and H_3-13/C-7 and -8 in the HMBC spectrum established the gross structure of compound **4**. The relative configurations of C-6 and C-7 in **4** was assigned to be *threo* form (6*S** and 7*S**) due to the coupling constant of mutually-coupled H-6 and H-7 ($J_{H\text{-}6/H\text{-}7}$ = 11.0 Hz) and compared with the literatures [28,29].

Compound **5** was obtained as yellow crystal, and was confirmed to have the molecular formula of $C_{14}H_{18}O_6$ as deduced from a pseudo-molecular ion $[M - H_2O + H]^+$ at *m/z* 265.1065 (calcd. 265.1076 for $C_{14}H_{17}O_5$) and a pseudo-molecular ion $[M - H_2O - H]^-$ at *m/z* 263.0927 (calcd. 263.0919 for $C_{14}H_{15}O_5$) in the positive ion mode and negative ion mode of HRESIMS, respectively, as supported by the analysis of ^{13}C NMR data (Table 1), indicating 6 degrees of unsaturation. The IR spectrum showed absorptions at 3400–2500 and 1658 cm^{-1}, indicating the presence of a conjugated carboxylic acid. Analysis of its ^1H NMR spectrum revealed the presence of three methyls at δ_H 2.01 (3H, d, $J = 2.0$, H_3-12), 2.13 (3H, s, H_3-13), and 2.46 (3H, dd, $J = 0.9$, 2.3 Hz, H_3-11), one methoxy at δ_H 3.83 (3H, s, OCH_3-10), and three olefinic protons at δ_H 6.21 (1H, q, $J = 2.3$ Hz, H-2), 6.42 (1H, s, H-7), and 7.11 (1H, brs, H-4) (Table 2). The ^{13}C NMR spectrum of **5** revealed 14 resonances for three methyls at δ_C 9.7 (C-13), 14.4 (C-12), and 19.5 (C-11), one methoxy at δ_C 56.9 (OCH_3-10), three olefinic methines at δ_C 95.4 (C-7), 123.2 (C-2), and 134.8 (C-4), and seven non-protonated carbons at δ_C 103.4 (C-9), 129.9 (C-5), 151.4 (C-3), 159.6 (C-6), 164.6 (C-10), 166.3 (C-8), and 169.3 (C-1). The postulated structure of **5** was confirmed by the HMBC correlations of H-2/C-1 and -4; H-4/C-5 and -6; H-7/C-5, -6, -8, and -9; H_3-11/C-2, -3, and -4; H_3-12/C-4, -5, and -6; H_3-13/C-8, -9, and -10; and OCH_3-10/C-10. Key correlations of H-2/H_3-12; H-4/H_3-11; and H-7/H_3-12 and -14 in the NOESY spectrum corroborated the configurations of $\Delta^{2(3)}$, $\Delta^{4(5)}$, $\Delta^{6(7)}$, and $\Delta^{8(9)}$ to be *E*, *E*, *Z*, and *E* forms, respectively.

The structure of 3-methylorsellinic acid (**6**) was elucidated by comparison with literature data [30]. 2-Furylhydroxymethylketone (**7**) was considered to be a potential strategy for producing cefuroxime as the second-generation cephalosporin antibiotic [31]. (+)-Pestalotiolactone A (**8**) was found to exhibit mild antimicrobial activities against *Vibrio anguillarum* QDIO-8 and *V. harveyi* QDIO-9 with the same MIC value of 32 μg/mL [32]. Cyclo[L-(4-hydroxyprolinyl)-L-leucine] (**9**) has ever been found to be a plant growth promoter [33]. Phenylacetic acid (**10**) exhibited moderate antimicrobial activities against *Ralstonia solanacearum* and *Escherichia coli* with MIC values of 25 and 150 μg/mL [34], respectively. *N*-acetyltyramine (**11**) was reported to reveal potent antimicrobial activities against many drug-resistant pathogens [35]. 4-Hydroxyphenylacetate (**12**) and methyl 4-hydroxyphenylacetate (**13**) are phenolic compounds, and have ever been isolated from cultures of a medicinal plant-derived fungus *Aspergillus flavipes* DZ-3 [36]. As the structural features classified by different culturing media, γ-lactone compounds **1**–**4** and **8** along with two polyketides **6** and **7**, aromatic compounds **10**–**13** together with a C_{13} polyketide **5**, and a cyclopeptide compound **9** were isolated from ME, PDB, and PDY groups, respectively.

Compounds **1**–**13** was assayed for anti-neuroinflammatory activity. The anti-neuroinflammatory activity of **1**–**13** was assessed by measuring the amount of nitric oxide (NO) production in lipopolysaccharide (LPS)-induced microglial BV-2 cells. Of all the tested compounds, **1** and **2** inhibited 45.6% and 41.8% of NO production (Fig. 4A), respectively, at a concentration of 20 μM without any cytotoxicity (Fig. 4B). The positive control curcumin exhibited 100% inhibition of NO production under the same concentration. In the literatures, compounds **6**, **7**, **11**, and **13** have also been evaluated their NO production inhibitory activities by employing *in vitro* cell culture platforms, and all their IC_{50} exceeded 50 μM which indicated relatively slight anti-inflammatory activities [37–40].

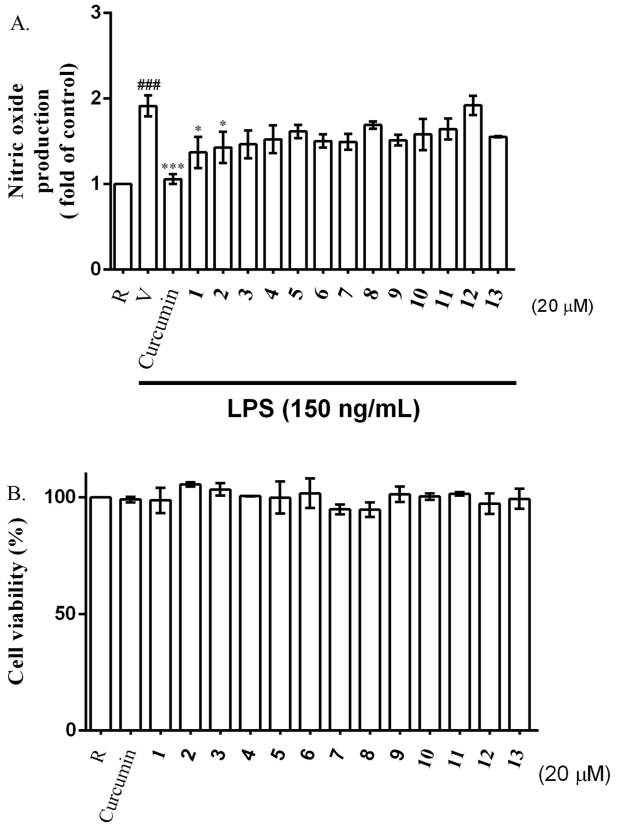

*Fig. 4. Effects of compounds **1**–**13** on LPS-induced NO production (A) in BV-2 microglial cells and their cytotoxicities (B). The concentration of test compounds was 20 μM. Data are expressed as the mean ± SD (n = 3). $^{###}p < 0.001$, compared with the resting group (R); $^{*}p < 0.05$, compared with the group of stimulation (V).*

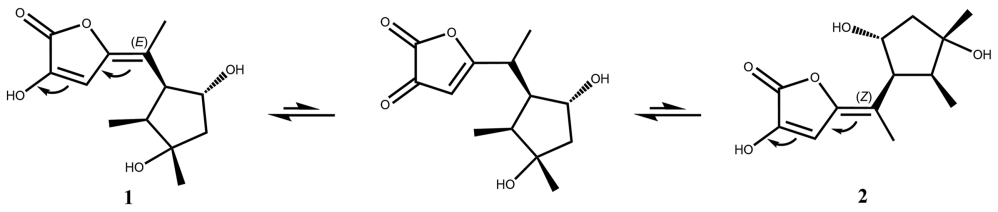

*Fig. 5. The tautomeric shifts of compounds **1** and **2**.*

In summary, the fungal strain *D. brachylaenae* Km1530 was cultured in three different media (PDY, ME, and PDB), and thirteen compounds **1**–**13**, including five previously undescribed polyketides, brachylactones A-D (**1**–**4**) and brachic acid (**5**), were isolated and identified from the fermented products. Of these, brachylactones A and B (**1** and **2**) were *E*/*Z*-tautomers, and they tautomerized readily in solution by the ratio of 3:2, respectively. In the previous report, it was pointed out that the γ-crotonolactone containing a conjugated exocyclic double bond was prone to tautomerize, and it was found when the exocyclic double bond contained a substituent, it had higher stereoselectivity for *E* form [41], the same as observed for compounds **1** and **2** in this report (Fig. 5). In view of the wide range of bioactive potential of lactone compounds [42–46], many other platforms should remain to be employed for further understanding the pharmacological properties of **1**–**4**. This is the first report to demonstrate the anti-neuroinflammatory activities of the C_{13} polyketides from *D. brachylaenae*.

Conflicts of interest

The authors declare no competing financial interest.

Acknowledgments

We thank Dr. His-Ching Tseng in the Instrumentation Center of the College of Science, National Taiwan University for the NMR data acquisition. This work was supported by grants from the National Science and Technology Council (NSTC 110-2320-B-002-023-MY3 and NSTC 113-2320-B-002-050-MY3) of Taiwan to T.-H.L.

References

[1] Hardoim PR, van Overbeek LS, Berg G, Pirttilä AM, Compant S, Campisano A, et al. The hidden world within plants ecological and evolutionary considerations for defining functioning of microbial endophytes. Microbiol Mol Biol R 2015;79:293–320.
[2] Strobel G, Daisy B. Bioprospecting for microbial endophytes and their natural products. Microbiol Mol Biol R 2003;67:491–502.
[3] Rodriguez RJ, White JF, Arnold AE, Redman RS. Fungal endophytes: diversity and functional roles. New Phytol 2009;182:314–30.
[4] Tan RX, Zou WX. Endophytes: a rich source of functional metabolites. Nat Prod Rep 2001;18:448–59.
[5] Nisa H, Kamili AN, Nawchoo IA, Shafi S, Shameem N, Bandh SA. Fungal endophytes as prolific source of phytochemicals and other bioactive natural products: a review. Microb Pathog 2015;82:50–9.
[6] Brakhage AA, Schroeckh V. Fungal secondary metabolites - strategies to activate silent gene clusters. Fungal Genet Biol 2011;48:15–22.
[7] Jia M, Chen L, Xin HL, Zheng CJ, Rahman K, Han T, et al. A friendly relationship between endophytic fungi and medicinal plants a systematic review. Front Microbiol 2016;7:906.
[8] Bethany KO, Mohammad RS. Antibiotic dialogues induction of silent biosynthetic gene clusters by exogenous small molecules. FEMS Microbiol 2017;41:19–33.
[9] Pfannenstiel BT, Keller NP. On top of biosynthetic gene clusters: how epigenetic machinery influences secondary metabolism in fungi. Biotechnol Adv 2019;37:107345.
[10] Giddings LA, Newman DJ. Extremophilic fungi from marine environments underexplored sources of antitumor, anti-infective and other biologically active agents. Mar Drugs 2022;20:62.
[11] Zhang XY, Tan XM, Yu M, Yang J, Sun BD, Qin JC, et al. Bioactive metabolites from the desert plant-associated endophytic fungus *Chaetomium globosum* (Chaetomiaceae). Phytochem 2021;185:112701.
[12] Carroll AR, Copp BR, Davis RA, Keyzers RA, Prinsep MR. Marine natural products. Nat Prod Rep 2021;38:362–413.
[13] Chang CH, Lee YC, Hsiao GR, Chang LK, Chi WC, Cheng YC, et al. Anti-epstein-barr viral agents from the medicinal herb-derived fungus *Alternaria alstroemeriae* Km2286. J Nat Prod 2022;85:2667–74.
[14] Chang CH, Hsiao GR, Wang SW, Yen JY, Huang SJ, Chi WC, et al. Chemical constituents from the medicinal herb-derived fungus *Chaetomium globosum* Km1226. Bot Stud 2023;64:34.
[15] Kaul S, Gupta S, Ahmed M, Dhar MK. Endophytic fungi from medicinal plants a treasure hunt for bioactive metabolites. Phytochem Rev 2012;11. 847–505.
[16] Muna AA, Josphat CM. Endophytes as producers of peptides an overview about the recently discovered peptides from endophytic microbes. Nat prod bioprospect 2014;4:257–70.
[17] Pan R, Bai XL, Chen JW, Zhang HW, Wang H. Exploring structural diversity of microbe secondary metabolites using OSMAC strategy a literature review. Front Microbiol 2019;10:294.
[18] Borkunov GV, Leshchenko EV, Berdyshev DV, Popov RS, Chingizova EA, Shlyk NP, et al. New piperazine derivatives helvamides B-C from the marine-derived fungus *Penicillium velutinum* ZK-14 uncovered by OSMAC (One Strain Many Compounds) strategy. Nat Prod Bioprospecting 2024;14:32.
[19] Le Loarer A, Dufosse L, Bignon J, Frederich M, Ledoux A, Fouillaud M, et al. OSMAC method to assess impact of culture parameters on metabolomic diversity and biological activity of marine-derived actinobacteria. Mar Drugs 2024;22:23.

[20] Hu ZX, Ye Y, Zhang YH. Large-scale culture as a complementary and practical method for discovering natural products with novel skeletons. Nat Prod Rep 2021;38: 1775−93.
[21] Hsiao G, Wang SW, Chiang YR, Chi WC, Kuo YH, Phong DA, et al. Anti-inflammatory effects of peptides from a marine algicolous fungus *Acremonium* sp. NTU492 in BV-2 microglial cell. J Food Drug Anal 2020;28:89−97.
[22] Lin FL, Ho JD, Cheng YW, Chiou GCY, Yen JL, Chang HM, et al. Theissenolactone C exhibited ocular protection of endotoxin-induced uveitis by attenuating ocular inflammatory responses and glial activation. Front Pharmacol 2018;9:326.
[23] Hsieh MH, Hsiao G, Chang CH, Yang YL, Ju YM, Kuo YH, et al. Polyketides with anti-neuroinflammatory activity from *Theissenia cinerea*. J Nat Prod 2021;84:1898−903.
[24] Jiang ZP, Su R, Chen MT, Li JY, Chen HY, Yang L, et al. *Ent*-eudesmane sesquiterpenoids with anti-neuroinflammatory activity from the marine-derived fungus *Eutypella* sp. F0219. Phytochem 2024;223:141221.
[25] Zhu SH, Chang YM, Li SW, Su MZ, Yao LG, Liang LF, et al. Exploring the chemical diversity of sesquiterpenes from the rarely studied south China sea soft coral *Sinularia tumulosa* assisted by molecular networking strategy. Phytochem 2024; 222:114110.
[26] Kong LQ, Wang YL, Tong Z, Dai RR, Yusuf A, Du LF, et al. Granulathiazole A protects 6-OHDA-induced Parkinson's disease from ferroptosis via activating Nrf2HO-1 pathway. Bioorg Chem 2024;147:107339.
[27] Yurchenko EA, Menchinskaya ES, Pislyagin EA, Trinh PTH, Ivanets EV, Smetanina OF, et al. Neuroprotective activity of some marine fungal metabolites in the 6-hydroxydopamin- and paraquat-induced parkinson's disease models. Mar Drugs 2018;16:457.
[28] Matsumori N, Kaneno D, Murata M, Nakamura H, Nakamura K. Stereochemical determination of acyclic structures based on carbon-proton spin-coupling constants. A method of configuration analysis for natural products. J Org Chem 1999;64:866−76.
[29] Besombes S, Robert D, Utille JP, Taravel FR, Mazeau K. Molecular modeling of syringyl and *p*-hydroxyphenyl β-O-4 dimers. Comparative study of the computed and experimental conformational properties of lignin β-O-4 model compounds. J Agri Food Chem 2003;51:34−42.
[30] Takenaka S, Seto S, Ojima N. Isolation of 2,4-dihydroxy-3,6-dimethylbenzoic acid (3-methylorsellinic acid) from a culture of aspergillus-terreus. J C S Chem Comm 1972:391−2.
[31] Zhang XH, Wei H, Wei XL, Qi TT, Zong XR, Liu ZX, et al. Biosynthesis of 2-furylhydroxymethylketone, an intermediate of cefuroxime, from furfural and formaldehyde using a ThDP-dependent enzyme. Green Chem 2023;25:4713−22.
[32] Li XD, Li XM, Yin XL, Li X, Wang BG. Antimicrobial sesquiterpenoid derivatives and monoterpenoids from the deep-sea sediment-derived fungus *Aspergillus versicolor* SD-330. Mar Drugs 2019;17:563.
[33] Cronan JM, Davidson TR, Singleton FL, Colwell RR, Cardellina JH. Plant growth promoters isolated from a marine bacterium associated with *Palythoa* sp. Nat Prod Lett 1998;11:271−8.
[34] Zhu YJ, Zhou HT, Hu YH, Tang JY, Su MX, Guo YJ, et al. Antityrosinase and antimicrobial activities of 2-phenylethanol, 2-phenylacetaldehyde and 2-phenylacetic acid. Food Chem 2011;124:298−302.
[35] Driche E, Badji B, Bijani C, Belghit S, Pont F, Mathieu F, et al. A new saharan strain of *Streptomyces* sp. GSB-11 produces maculosin and N-acetyltyramine active against multidrug-resistant pathogenic bacteria. Curr Microbiol 2022;79:298.
[36] Liu W, Liu Y, Yang F, Han SY, Zhang J, Yang H, et al. Asperflaloids A and B from *Aspergillus flavipes* DZ-3, an endophytic fungus of *Eucommia ulmoides* Oliver. Molecules 2021;26:3514.
[37] Zhang X, Liu LY, Huang JN, Ren XT, Zhang GJ, Che Q, et al. Genome mining-guided discovery of two new depsides from *Talaromyces* sp. Mar Drug 2025;23:130. HDN1820200.
[38] Wang YH, Ding LZ, Hu Q, Wang C. New natural furfural derivatives from the leaves and stems of *Pogostemon cablin*. Nat Prod Res 2023;37:434−40.
[39] Woo KW, Kwon OW, Kim SY, Choi SZ, Son MW, Kim KH, et al. Phenolic derivatives from the rhizomes of *Dioscorea nipponica* and their anti-neuroinflammatory and neuroprotective activities. J Ethnopharmacol 2014;155:1164−70.
[40] Qiu CY, Tong L, Yuan T, Wang F, Zhao F, Chen LX. Constituents from Vitex negundo var. heterophylla and their inhibition of nitric oxide production. J Nat Med 2017;71: 292−8.
[41] Langer P, Schneider T, Stoll M. Domino reaction of 1-3-bis (trimethylsilyloxy)-1,3-dienes with oxalyl chloride General and stereoselective synthesis of γ-alkylidenebutenolides. Chem Eur J 2000;6:3204−14.
[42] Sartori SK, Diaz MAN, Diaz-Muñoz G. Lactones Classification, synthesis, biological activities, and industrial applications. Tetrahedron 2021;84:132001.
[43] Shen WY, Mao HQ, Huang Q, Dong JY. Benzenediol lactones a class of fungal metabolites with diverse structural features and biological activities. Eur J Med Chem 2015;97: 747−77.
[44] Kim Y, Sengupta S, Sim T. Natural and synthetic lactones possessing antitumor activities. Int J Mol Sci 2021;22:1052.
[45] Surowiak AK, Balcerzak L, Lochynski S, Strub DJ. Biological activity of selected natural and synthetic terpenoid lactones. Int J Mol Sci 2021;22:5036.
[46] Mazur M, Skrobiszewski A, Gladkowski W, Podkowik M, Bania J, Nawrot J, et al. Lactones 47. Synthesis, antifeedant and antibacterial activity of γ-lactones with *p*-methoxyphenyl substituent. Pest Manag Sci 2016;72:489−96.